Non-equilibrium structure of the vapor-liquid interface of a binary fluid

Aldo Frezzotti

Dipartimento di Matematica del Politecnico di Milano - Piazza Leonardo da Vinci 32 - I20133 Milano - Italy

Abstract. The evaporation of a binary liquid mixture of monatomic species into near vacuum has been investigated by molecular dynamics simulations. It has been assumed that atomic interaction forces can be derived by Lennard-Jones potentials. Results are presented about surface composition changes induced by evaporation, the shape of the distribution functions of evaporating atoms. Estimates of evaporation coefficients are given.

Keywords: mixtures, evaporation, molecular dynamics
PACS: 51.10.+y,64.70.fm

INTRODUCTION

A relatively small number of studies have investigated the structure of the one-dimensional Knudsen layer which forms in the vapor phase above the liquid surface during the evaporation of a binary substance[1, 2, 3]. The common basis of these investigations is the following system of coupled, steady and spatially one-dimensional Boltzmann equations[4]:

$$v_x \frac{\partial f_i}{\partial x} = \sum_{j=1}^{2} Q_{ij}(f_i, f_j) \quad i = 1,2 \tag{1}$$

$f_i(x, \mathbf{v})$ being the distribution function of molecular velocities $\mathbf{v}$ of species i at the spatial location x, whereas $Q_{ij}(f_i, f_j)$ is the collision integral representing the interaction between species i and j. Eqs.(1) have been solved by a variety of techniques, ranging from moment methods[1] to DSMC simulations[2] and deterministic schemes for the linearized form of the equations[3]. Since the main aim of the studies mentioned above was understanding the gas dynamics in the vapor kinetic region, the simplest form of boundary conditions at the vapor-liquid interface was adopted. Accordingly, Eqs. (1) were solved assuming that following boundary conditions hold at the evaporating surface located at $x = 0$:

$$f_i(0, \mathbf{v}) = \frac{n_{wi}}{(2\pi R_i T_w)^{3/2}} \exp\left(-\frac{\mathbf{v}^2}{2R_i T_w}\right) \qquad , v_x > 0 \tag{2}$$

In Eq. (2) T_w is the surface temperature whereas n_{wi} is the saturated vapor density of the $i-th$ species at temperature T_w. As is clear from Eq. (2), a unit evaporation coefficient was assumed for both species. Moreover, both the surface temperature T_w and the partial vapor densities n_{wi} were kept constant. Both assumptions present problematic aspects which deserve a deeper analysis.

In the case of a mono-component fluid, the functional form of the distribution function of evaporating molecules and the determination of evaporation coefficients has been the subject of several investigations based on molecular dynamics (MD) simulations [5, 6, 7] and mean field approximations of simple liquids[8]. The results show that the half-range Maxwellian specified by Eq. (2) provides a good approximation of simulation results, in the case of near vacuum evaporation. However, all simulation methods predict evaporation coefficients slightly below unit. Deviations from the functional form of Eq. (2) have been reported in presence of a significant molecular flux impinging on the liquid surface [9].

Considering constant surface properties and a steady analysis of the vapor flow in the Knudsen layer is not unreasonable. As a matter of fact, changes of the liquid surface physical conditions *might* be slow when compared with the characteristic kinetic time scales in the vapor. However, the steady analysis predicts that, as expected, the net number fluxes ϕ_i of the two vapor components are not the same, the difference being determined by the species mass ratio. Hence, evaporation should cause a continuous change in the surface composition of the condensed phase. In the light of the considerations expressed above, the research work described in the present paper aims at improving

the boundary conditions to be used at the vapor liquid interface of a multi-component fluid. Following the research lines of the single component case, the near vacuum evaporation of a liquid mixture of two monatomic species has been studied by non-equilibrium MD simulation, in order to obtain the form of the distribution function of evaporating molecules as well as estimates of evaporation coefficients following the surface composition time evolution.

EQUILIBRIUM MD SIMULATIONS AND PHASE COEXISTENCE DATA

Equilibrium and non-equilibrium classical MD simulations[10] of a binary liquid in contact with its vapor phase have been performed on system of atoms belonging to two different species characterized by atomic masses m_1 and m_2, respectively. It is assumed that atoms of species a ($a = 1,2$) interact pairwise with atoms of species b ($b = 1,2$) through forces derived from the following Lennard-Jones potential

$$\phi_{ab}(\rho) = 4\varepsilon_{ab}\left[\left(\frac{\sigma_{ab}}{\rho}\right)^{12} - \left(\frac{\sigma_{ab}}{\rho}\right)^{6}\right] \tag{3}$$

being ρ the distance between two interacting atoms. As is well known, ε_{ab} is the depth of the potential well, whereas $\rho = 2^{1/6}\sigma_{ab}$ is the position of the potential minimum. The quantities m_1, σ_{11} and $\sigma_{11}\sqrt{\frac{m_1}{\varepsilon_{11}}}$ have been adopted as reference mass, length and time units, respectively. In all simulations described below, the following set of non-dimensional parameters has been adopted

$$\begin{aligned} m_2 &= 2.0977 \\ \sigma_{12} &= 1.0330396, \quad \sigma_{22} = 1.0660793 \\ \varepsilon_{12} &= 1.1668058, \quad \varepsilon_{22} = 1.3614357 \end{aligned}$$

The parameters choice has been dictated by the availability of a number of previous studies of the phase coexistence diagram of Argon-Krypton mixtures, based on the same (or similar) parameters set[11]. The dimensionless values given above have been obtained by selecting Argon as reference species and applying Lorentz-Berthelot mixing rule[10]

$$\sigma_{12} = \frac{\sigma_{11} + \sigma_{22}}{2} \tag{4}$$

$$\varepsilon_{12} = \sqrt{\varepsilon_{11}\varepsilon_{22}} \tag{5}$$

to compute cross interaction parameters.

The system dynamics has been obtained by computing the motion of a few thousand atoms in parallelepipedal box of sides L_x, L_y and L_z. To simulate an infinite system, periodic boundary conditions have been applied along x and y directions which are parallel to the liquid surface. When simulating systems in equilibrium, periodic boundary conditions have also been applied along z direction, normal to the vapor-liquid interface. Newton's equations have been integrated numerically by a simple velocity Verlet scheme[10]. Forces have been computed following the minimum image convention[10] and truncating atomic interactions when the relative distance ρ exceeded a specified truncation radius ρ_c. Atoms have also been sorted into a cell system, in order to make the search of nearest neighbors more efficient.

The knowledge of the phase coexistence diagram of the binary fluid is of fundamental importance for the interpretation of non-equilibrium simulations. The equilibrium properties of the liquid-vapor system in binary mixtures has been extensively investigated by Monte Carlo, Gibbs ensemble Monte Carlo and MD methods[11]. However, the results for a specific system slightly depend on the adopted numerical technique and computational parameters. In particular, the choice of the truncation radius ρ_c strongly affects phase coexistence data[11]. Therefore a few reference points of the phase coexistence diagram have been computed afresh by running a number of equilibrium MD simulations at constant atom numbers N_i, total volume $V = L_x L_y L_z$ and temperature T. The desired temperature level has been obtained by a simple Gaussian thermostat[10]. Reference equilibrium results have been obtained for three values of the reduced temperature $T^* = \frac{k_B T}{\varepsilon_{11}}$, being k_B the Boltzmann constant. For each temperature value, three different system compositions have been considered by assigning the overall Argon (species 1) concentration $\bar{x}_1 = N_1/(N_1 + N_2)$. As shown below, a more refined composition resolution has been obtained for the special case $T^* = 0.8$. In order to keep

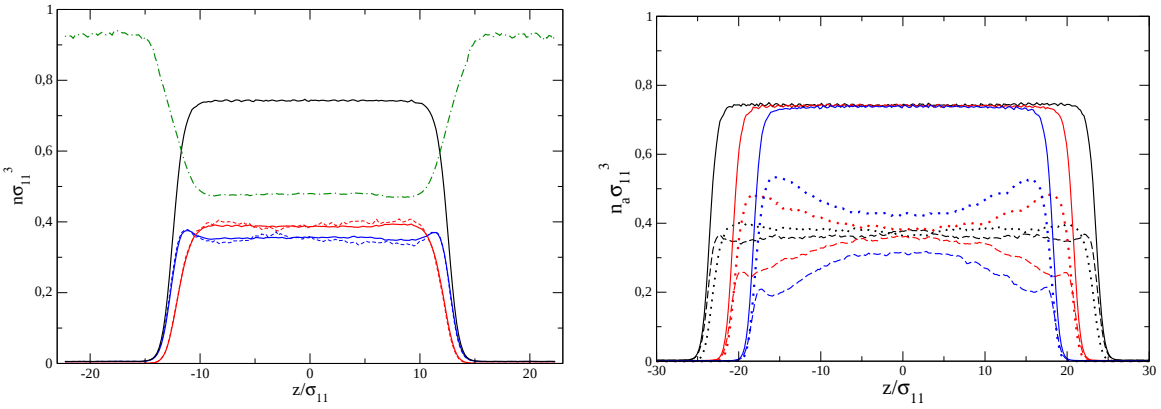

FIGURE 1. **Left**- Equilibrium density and concentration profiles. $T^* = 0.8$, $\bar{x}_1 = 0.5$. Solid lines represent averaged data over six independent runs: (black) total reduced density $n\sigma_{11}$; (blue) $n_1\sigma_{11}$; (red) $n_2\sigma_{11}$. Blue dot-dashed line represents averaged Argon concentration, $x_1 = n_1/n$. Dashed lines represent single run density profiles. **Right**- Evaporation into near vacuum. Time evolution of total and partial densities profiles. Color indicates time level: $t = 2 \times 10^2$ (black); $t = 2 \times 10^3$ (red); $t = 4 \times 10^3$ (blue). Solid lines: total number density , $n\sigma_{11}^3$; dashed lines: number density of species 1 ; dotted lines: number density of species 2.

the computational effort within acceptable limits, in view of non-equilibrium simulations, the truncation radius ρ_c has been set equal to $3\sigma_{22}$. The simulation box dimensions L_x, L_y and L_z have been set equal to $8\rho_c$, $8\rho_c$ and $14\rho_c$, respectively, whereas the dimensionless time step has been set equal to 0.005. The total number of atoms was varied between 8000 and 12000. Each simulation has been started from an initial system configuration in which atoms are located at the corners of a simple cubic lattice with random velocities sampled from a Maxwellian with zero mean velocity and temperature equal to T^*. Then, the system dynamics is followed for 400000 time steps. Time averaged macroscopic quantities are obtained from the last 100000 time steps. Test computations have been successfully compared with the results in Ref.[11] by setting the truncation radius ρ_c equal to $4.4\sigma_{22}$. Density and concentration profiles are shown in Figure 1 for the case $T^* = 0.8$, $\bar{x}_1 = 0.5$. The total number density profile $n(z)$ quickly reaches its final shape and exhibits very little run to run variations, as shown by the standard deviation associated with the total liquid and vapor densities ($n^{(l)}$ and $n^{(v)}$)) reported in Table1. Partial densities profiles are less uniform in the liquid region and disuniformities exhibit both a longer life time and a larger run to run variation[11]. Smoothed density profiles have been obtained by averaging the results of six independent runs. The equilibrium partial and total liquid and vapor densities reported in Table 1 have been obtained by spatial averages of density profiles in the vapor and liquid bulk regions. As is clear from the interaction parameters setting, Argon is the more volatile species. The system composition is not constant, the vapor being Argon rich. It is also worth observing that Argon is adsorbed on the liquid surface[11], as it can be seen from the relative displacement of Argon and Krypton density profiles and the Argon density local maxima in proximity of the vapor liquid interface.

NON-EQUILIBRIUM MD SIMULATIONS

After obtaining the necessary reference points on the phase coexistence diagram, a series of non-equilibrium MD simulations has been performed to study the evaporation of the liquid in near vacuum conditions. As noted in previous investigations[5], in these numerical experiments the back scattered vapor component is virtually absent. Hence it is possible to obtain the shape of the distribution function of evaporating molecules as well as evaporation coefficients estimates. MD simulations have been performed by the same general numerical method used for equilibrium simulations. However, following previous studies[6, 8], periodic boundary conditions along z direction have been replaced with a simple open end condition which removes from the simulation box those atoms whose distance from the receding vapor-liquid interface exceeds a specified threshold. The distance should be large enough not to influence the interface structure, but small in comparison with the vapor mean free path λ_v. In non-equilibrium simulations, the thermostat has been applied only in a central strip of the liquid slab. The strip thickness has been gradually reduced in time following the interface motion. Each simulation has been started from a specified equilibrium condition in

TABLE 1. Equilibrium liquid and vapor densities as a function of reduced temperature $T^* = k_b T/\varepsilon_{11}$ and overall species 1 composition $\bar{x}_1$. $n_i^{(l)}\sigma_{11}^3$ is the reduced density of species i in the liquid phase; $n_i^{(v)}\sigma_{11}^3$ is the reduced density of species i in the vapor phase; $x_1^{(l)}$ and $x_1^{(v)}$ are the liquid and vapor concentrations of species 1. Standard errors associated with reduced densities are written below each value.

T^*	$\bar{x}_1$	$n_1^{(l)}\sigma_{11}^3$	$n_2^{(l)}\sigma_{11}^3$	$n^{(l)}\sigma_{11}^3$	$x_1^{(l)}$	$n_1^{(v)}\sigma_{11}^3$	$n_2^{(v)}\sigma_{11}^3$	$n^{(v)}\sigma_{11}^3$	$x_1^{(v)}$
0.8	0.25	0.171	0.556	0.7278	0.235	0.0026	6.0e-04	0.0032	0.812
		±2.5e-03	±2.2e-03	±4.0e-04		±1.5e-04	±1.0e-04	±2.1e-04	
0.8	0.50	0.356	0.387	0.7428	0.479	0.0054	4.4e-04	0.0058	0.923
		±4.4e-03	±4.2e-03	±3.0e-04		±3.0e-04	±1.3e-04	±4.0e-04	
0.8	0.75	0.554	0.201	0.7553	0.733	0.0086	3.0e-04	0.0089	0.967
		±5.0e-03	±5.0e-03	±4.0e-04		±5.0e-04	±0.9e-05	±5.0e-04	
0.9	0.25	0.162	0.535	0.6965	0.232	0.0055	1.9e-03	0.0074	0.746
		±4.0e-03	±3.0e-03	±4.6e-04		±3.2e-04	±2.0e-04	±4.0e-04	
0.9	0.50	0.336	0.370	0.7065	0.476	0.0113	1.4e-03	0.0127	0.888
		±2.9e-03	±2.8e-03	±4.2e-04		±4.6e-04	±1.4e-04	±5.0e-04	
0.9	0.75	0.519	0.193	0.7113	0.729	0.0187	9.0e-04	0.0196	0.954
		±4.5e-03	±4.5e-03	±7.0e-04		±8.0e-04	±1.5e-04	±8.0e-04	
1.0	0.25	0.152	0.512	0.6633	0.229	0.0092	4.7e-03	0.0138	0.663
		±2.0e-03	±1.9e-03	±2.4e-04		±4.2e-04	±2.7e-04	±6.3e-04	
1.0	0.50	0.312	0.355	0.6674	0.468	0.0205	3.7e-03	0.0243	0.847
		±4.3e-03	±4.3e-03	±4.8e-04		±7.3e-04	±2.4e-04	±9.3e-04	
1.0	0.75	0.481	0.182	0.6634	0.725	0.035	2.4e-03	0.0372	0.936
		±1.8e-03	±1.2e-03	±6.9e-04		±1.4e-03	±1.7e-04	±1.3e-03	

which the liquid slab thickness has been set approximately equal to $50\sigma_{11}$. The simulation box section area $S = L_x L_y$ has been set equal to $36\rho_c^2$. Large initial slab thickness and box section area are necessary to run sufficiently long simulations and collect enough atoms in the vapor phase to compute the quantities of interest. The results presented here have been obtained by following the evolution of the initially equimolar system ($\bar{x}_1 = 0.5$) at $T^* = 0.8$, the initial total number of atoms being equal to 13660. The temperature value has been selected as a compromise between the two contrasting needs of having a rarefied vapor and a sufficient number of atoms of both species in the vapor phase. In the condition specified above the ratio $\frac{\lambda_v}{\sigma_{11}}$ is of the order of $\frac{1}{n^{(v)}\sigma_{11}^3}$ which, according to Table 1, takes the value 1.7×10^2 whereas the average atomic distance in the vapor phase is $\sqrt[3]{\frac{1}{n^{(v)}\sigma_{11}^3}} \approx 5.6$, about twice the value of the truncation radius ρ_c. Total and partial densities snapshots at dimensionless times $t = 200,\ 2000,\ 4000$ are shown in Figure 1. During evaporation, the total density profile recedes while keeping almost constant shape. In the prescribed conditions, the evaporation rate is small, therefore the temperature difference between the thermostatted central slab region and the liquid surface is of the order of 0.02 in reduced units. The preferential evaporation of Argon causes a continuous change of the system composition both in the liquid and in the vapor phase, as expected. In particular the surface composition becomes Krypton rich, whereas the Argon density profile in the interface region keeps the local maxima already observed in equilibrium simulations. The distribution functions of evaporating atoms has been obtained by recording events of atoms crossing two control surfaces located in the vapor region at a distance of $3\sigma_{11}$ from the interfaces, whose positions have been obtained from the maximum slope of the total density profile. As shown in Figure 2, the normalized reduced distribution functions of velocity components normal and parallel to the liquid surface are well approximated by Maxwellians having the liquid bulk temperature, as found for a mono-component fluid in similar conditions[5, 6, 8]. The evaporation coefficients α_i of the two evaporating species have been obtained from the expression:

$$\phi_i = \alpha_i n_i^{(eq)}(T_s, x_s)\sqrt{\frac{k_B T_s}{2\pi m_i}} \tag{6}$$

In Eq. 6, ϕ_i is the evaporating flux of species i in free molecular regime, T_s and x_s are the surface temperature and Argon concentration, respectively. The quantity $n_i^{(eq)}$ is the equilibrium vapor density of species i at temperature T_s and liquid concentration x_s. The fluxes ϕ_i have been obtained from the MD simulation by recording the numbers $N_i^{(out)}(t)$ of atoms of species i removed from the domain after crossing a control surface placed at a distance d_r of $5\sigma_{11}$ from the receding interfaces. Simulations with larger values of d_r did not show appreciable changes of $N_i^{(out)}(t)$ histories, thus confirming

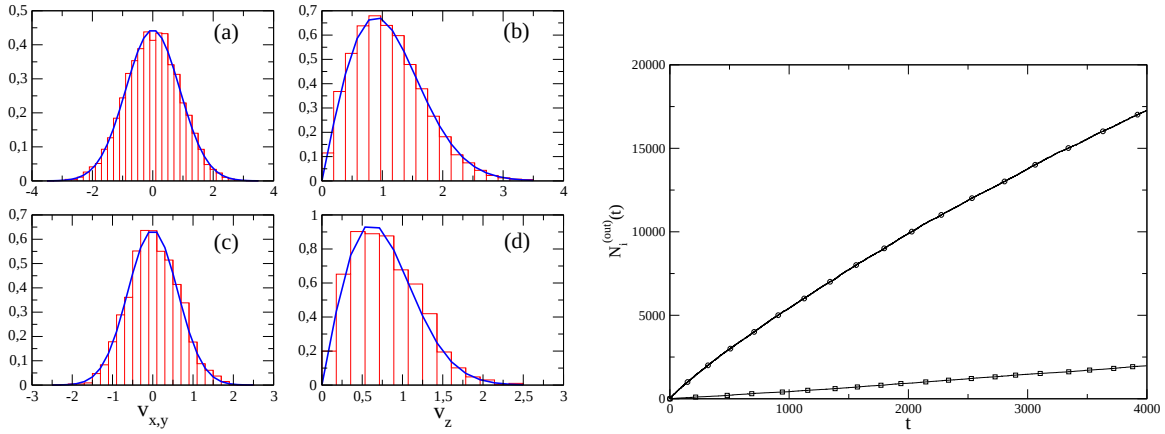

FIGURE 2. **Left** - Reduced normalized distribution functions of evaporating atoms: (a) Argon $f_{x,y}(v_{x,y})$; (b) Argon $v_z f_z(v_z)$; (c) Krypton $f_{x,y}(v_{x,y})$; (d) Krypton $v_z f_z(v_z)$. Solid lines: Maxwellian distributions at $T^* = 0.8$. **Right** - Time histories of number of evaporated atoms $N_i^{(out)}(t)$ (superposition of six independent MD simulations)

the assumption of nearly free molecular flow in the vapor. As shown in Figure 2, fluxes are not constant because of the surface composition change. The Argon flux decreases, whereas the Krypton flux increases. The equilibrium vapor densities $n_i^{(eq)}$ have been obtained by setting $T_s = 0.8$ and by assigning to x_s the instantaneous value taken by Argon concentration at the spatial location just behind the local density maxima in proximity of the vapor-liquid interface. This choice is based on the assumption that such position marks out the beginning of a quasi-equilibrium region whose properties could be described by hydrodynamic equations for the liquid phase. More precisely, the time history of $x_s(t)$ has been obtained from non-equilibrium simulations. For each value of the liquid phase composition $x_s(t)$, the corresponding equilibrium partial vapor densities $n_i^{(eq)}$ have been obtained by applying a simple cubic interpolation to the data in Table 2 which contains points on the system coexistence diagram at $T^* = 0.8$ with a greater resolution on composition.

TABLE 2. Equilibrium system at $T^* = 0.8$. Vapor density and composition as a function of liquid composition

$\bar{x}_1$	$x_1^{(v)}$	$x_1^{(l)}$	$n_1^{(v)}\sigma_{11}$	$n^{(v)}\sigma_{11}^3$
0.125	0.114	0.660	0.720	0.0019
0.250	0.235	0.812	0.7278	0.0032
0.375	0.356	0.884	0.7360	0.0045
0.50	0.479	0.923	0.7428	0.0058

The evaporation coefficients α_i are then obtained by computing the fluxes ϕ_i by differentiating polynomial fits of $N_i^{(out)}$ data shown in Figure 2. Time histories of surface composition $x_s(t)$ and evaporation coefficients are presented in Table 3.

The numerical results seem to indicate that the evaporation coefficients are not the same for the two species. The evaporation coefficient of Argon appears to be slightly below the value obtained by MD simulations of evaporation of a mono-component LJ fluid, whereas the evaporation coefficient of the less volatile species is slightly above the mono-component value. The results also show a surface concentration dependence of evaporation coefficients. This is not unreasonable, since surface composition determines local bonding atomic forces. However the results presented in Table 3 are potentially affected by a few error sources, like, for instance the numerical differentiation of noisy $N_i^{(out)}$ data used to estimate instantaneous fluxes.

TABLE 3. Evaporation into near vacuum. System initial reduced temperature $T^* = 0.8$, initial overall composition $\bar{x}_1 = 0.5$. Time histories of surface composition $x_s(t)$ and evaporation coefficients

$t\frac{1}{\sigma_{11}}\sqrt{\frac{\varepsilon_{11}}{m_1}}$	$x_s(t)$	α_1	α_2
1000	0.382	0.72	0.85
2000	0.335	0.70	0.90
3000	0.295	0.71	0.87
4000	0.265	0.75	0.82

CONCLUSIONS

The evaporation of a binary liquid into near vacuum has been investigated by molecular dynamics simulations. Numerical experiments have been limited to fluid temperature and composition values which give rise to a dilute vapor phase. The time evolution of the liquid bulk and interface region has been obtained. The distribution functions of evaporating atoms and evaporation coefficients have been obtained. The results confirm previous findings about the single component system, suggesting that a half-range Maxwellian with zero drift velocity and temperature equal to the liquid surface temperature is a good approximation of emitted atoms distribution functions shape, in the simulation conditions. The computations of evaporation coefficients is more delicate than in the single component case. The present results are still based on a small number of simulations, hence they have to be considered as preliminar till the influence of all the possible error sources has been fully assessed.

ACKNOWLEDGMENTS

The author gratefully acknowledges the support received from *Fondazione Cariplo* within the framework of the project *Surface Interactions in micro/nano devices*

REFERENCES

1. A. Frezzotti, "Kinetic Theory Study of the Strong Evaporation of a Binary Mixture," in *Proceedings of the 15th International Symposium on Rarefied Gas Dynamics*, edited by V. Boffi, and C. Cercignani, B.G. Teubner Stuttgart, 1986, vol. 2, pp. 313–322.
2. A. Frezzotti, "Kinetic theory description of the evaporation of multi-component substances," in *Rarefied Gas Dynamics 20*, edited by C. Shen, Peking University Press, 1997, pp. 837–846.
3. S. Yasuda, S. Takata, and K. Aoki, *Physics of Fluids* **17**, 047105 (2005).
4. C. Cercignani, *The Boltzmann Equation and Its Applications*, Springer-Verlag, Berlin, 1988.
5. V. V. Zhakhovskii, and S. I. Anisimov, *JETP* **84** (1997).
6. T. Ishiyama, T. Yano, and S. Fujikawa, *Phys. Fluids* **16**, 2899 (2004).
7. R. Meland, A. Frezzotti, T. Ytrehus, and B. Hafskjold, *Phys. Fluids* **16**, 223 (2004).
8. A. Frezzotti, L. Gibelli, and S. Lorenzani, *Phys. Fluids* **17**, 012102 (2005).
9. T. Ishiyama, T. Yano, and S. Fujikawa, *Phys. Rev. Lett.* **95**, 084504 (2005).
10. M. Allen, and D. Tildesley, *Computer Simulation of Liquids*, Clarendon Press, 1989.
11. C. D. Holcomb, P. Clancy, and J. Zollweg, *Molecular Physics* **78** (1993).